

## A multifractal study of wave functions in 1-D quasicrystals

G ANANTHAKRISHNA\* and VIJAY KUMAR

Materials Science Division, Indira Gandhi Centre for Atomic Research, Kalpakkam 603 102, India

\*Present and permanent address: Materials Research Centre, Indian Institute of Science, Bangalore 560 012, India

MS received 11 June 1990; revised 30 November 1990

**Abstract.** Using multifractal analysis we study extended, self-similar and non-self-similar type of wave functions in the Fibonacci model. Extended states arising due to commutation of transfer matrices for certain blocks of atoms in quasiperiodic systems are shown to have the same signature as the Bloch states in terms of the singularity spectrum with  $f(\alpha) = \alpha = 1$ . Numerically, however, the extended states show a typical multifractal behaviour for finite chain lengths. Finite size scaling corrections yield results consistent with that obtained analytically. The self-similar states at the band edges show a multifractal behaviour and they are energy dependent in the case of blocks of atoms arranged in a Fibonacci sequence. For non-self-similar states we obtain a non-monotonic behaviour of  $f(\alpha)$  as a function of the chain length. We also show that in cases where extended states exist, the cross-over from extended to non-self-similar states is gradual.

**Keywords.** Multifractal; singularity spectrum; self-similar wave functions; quasicrystal; Fibonacci chain.

PACS Nos 71·50; 71·20; 71·30; 05·45

### 1. Introduction

In recent years the spectrum of the one-dimensional tight binding model on a Fibonacci sequence (FS) has been widely studied as a model for the electronic structure of quasiperiodic systems (eg Kohmoto *et al* 1983; Ostlund *et al* 1983; Nori and Rodrigues 1986; Valsakumar and Ananthakrishna 1987; Kohmoto *et al* 1987). It is known to exhibit a singular continuous spectrum (Delyon and Petritis 1986; Suto 1989). However, much less attention has been paid to the study of the wave functions in quasiperiodic systems. The wave functions corresponding to the singular continuous spectrum called critical, are neither localized nor extended and have a rich variety of interesting behaviour which is not properly explored. Several authors have used multifractal analysis (Hentschel and Procaccia 1983; Halsey *et al* 1986) to study the extended, localized and self-similar wave functions which arise in quasiperiodic structures (Siebesma and Pietronero 1987; Pietronero *et al* 1987; Mato and Caro 1987; Evanagelu 1987). However, none of these studies address the problem of estimating finite size effects of  $f(\alpha)$  spectrum. Recent studies (Fujiwara *et al* 1989; Hiramoto and Kohmoto 1989) do incorporate finite size scaling corrections properly in the case of self-similar, localized and extended wave functions. Fujiwara *et al* (1989) also show that infinite chain behaviour of  $f(\alpha)$  spectrum is difficult to obtain for non-self-similar wave functions. These states correspond to bounded chaotic orbits

of the trace map (Kohmoto *et al* 1987). For this reason, we will hereafter refer to such states as chaotic states (Kohmoto *et al* 1987; Fujiwara *et al* 1989).

Contrary to the general belief (eg Hiramoto and Kohmoto 1989) that all the states in the Fibonacci model are critical, extended like states with quasiperiodic amplitude can also arise (Kumar and Ananthakrishna 1987; Ananthakrishna and Kumar 1988; Ananthakrishna 1989; Kumar 1990a, b). They correspond to energies  $E_{ex}$  for which the transfer matrices of blocks of atoms commute. Such states can arise in other quasiperiodic sequences also (Ananthakrishna 1990). The characterization of these states and the states in their vicinity would be of interest because: (1) it is known that most of the other states are non-self-similar or chaotic (Kohmoto *et al* 1987) and so a cross-over from extended to chaotic states should occur and (2) if there is a finite density of states in the vicinity of the ES which behave similar to the ES the physical properties of quasiperiodic structures could be very different. In this paper we present a detailed study of the critical and extended types of wave functions of a FS using the multifractal analysis. In §2, we first recapitulate the essential results on wave functions. In §3A, after summarizing the multifractal method, we show analytically\* that the quasiperiodic extended type wave functions have the same signature as the Bloch states with  $f(\alpha) = \alpha = 1$ . In §3B, we present numerical results coupled with finite size scaling for the extended states. We find a spectrum of scaling indices  $f(\alpha)$  much like multifractals even for very large chain lengths, suggesting dominant finite size scaling corrections. The limiting value thus obtained is consistent with the analytical result. Due to the existence of such states, there is a finite density of neighbouring states which behave like ES with  $f(\alpha) = \alpha = 1$ . We demonstrate that as we go away from  $E_{ex}$  there is a lack of convergence as a function of the size of the system and this cross-over occurs gradually. *The nonmonotonic behaviour of  $f(\alpha)$  as a function of the size of system holds true for an arbitrary non-self-similar or chaotic wave function.* Thus, we consider the lack of convergence as the signature of the chaotic state. These results are further corroborated by the corresponding Poincare maps of the wave function (§3D). Section 3C contains results on self-similar states at band edges for chains with both single and blocks of two atoms. We find energy dependent scaling behaviour for the case with two atoms per block in contrast to a single type for one atom per block. Summary and discussion are presented in §4.

## 2. Wave functions

We consider the tight binding model

$$E\psi_n = t_{nn+1}\psi_{n+1} + t_{nn-1}\psi_{n-1} + \varepsilon_n\psi_n \quad (1)$$

on a FS where  $\varepsilon_n = \varepsilon_A$  or  $\varepsilon_B$  and  $t_{nn+1} = t$  (chosen for simplicity). Then, we have

$$\begin{pmatrix} \psi_{n+1} \\ \psi_n \end{pmatrix} = \mathbf{T}_n \begin{pmatrix} \psi_n \\ \psi_{n-1} \end{pmatrix} \quad (2)$$

\*A short report of this result has been published earlier (Ananthakrishna 1990).

where

$$\mathbf{T}_n = \begin{pmatrix} \frac{E - \varepsilon_n}{t_{nn+1}} & -\frac{t_{nn-1}}{t_{nn+1}} \\ 1 & 0 \end{pmatrix} \quad (3)$$

Let  $\mathbf{T}_A$  and  $\mathbf{T}_B$  be the transfer matrices corresponding to the  $A$  and  $B$  sites. The energy spectrum for a FS with one atom or block of atoms on each site in this model has been discussed by us previously (Kumar and Ananthakrishna 1987; Ananthakrishna and Kumar 1988). For the sake of completeness we recapitulate some of the essential results here. If there are  $N(M)$  atoms in the  $A(B)$  block, then the corresponding block transfer matrices are  $\tau_A(\tau_B)$ . Defining  $\mathbf{M}_r$  to be the transfer matrix for the  $r$ th FS with  $F_r$  ( $r$ th Fibonacci number) blocks of atoms and  $X_r = (1/2)\text{Tr}\mathbf{M}_r$ , then  $\mathbf{M}_r = \mathbf{M}_{r-2}\mathbf{M}_{r-1}$  and  $X_r$  obeys a trace map for which  $I = X_{r+1}^2 + X_r^2 + X_{r-1}^2 - 2X_{r+1}X_rX_{r-1} - 1$ , is an invariant. For  $N = M = 1$ ,

$$I = (\varepsilon_B - \varepsilon_A)^2/4t^2 \quad (4)$$

and there is no ES. For the present case, the wave functions for the band centers, edges and other energies have features similar to those obtained in the case of the off-diagonal model by Kohmoto *et al* (1987). The existence of the resonant states can be found by demanding the commutation of the transfer matrices corresponding to two distinct blocks of atoms not necessarily belonging to  $A$  or  $B$  type exclusively. In the case when blocks of identical atoms are used, (i.e.  $N > 1$  and  $M > 1$ ) it was shown (Ananthakrishna and Kumar 1988) that corresponding to  $\mathbf{T}_A^N = \pm \mathbf{I}$  or  $\mathbf{T}_B^M = \pm \mathbf{I}$ , there are specific energies at which the wave function has a form of an ES. Considering  $N = M = 2$ ,

$$I = w^2(w^2 - 4E^2)^2/64t^6, \quad (5)$$

where  $\varepsilon_B = -\varepsilon_A = w/2$ . For  $E = E_{\text{ex}}$ ,  $I$  vanishes and here we find  $E_{\text{ex}} = \pm w/2$ . Taking  $E = w/2$ , we have

$$\mathbf{T}_A = \begin{pmatrix} -\frac{w}{|t|} & -1 \\ 1 & 0 \end{pmatrix} \quad \text{and} \quad \mathbf{T}_B = \begin{pmatrix} 0 & -1 \\ 1 & 0 \end{pmatrix}. \quad (6)$$

The wave function at a site  $s = 2k + 2p$  with  $2k - B$  sites and  $2p - A$  sites is given by

$$\begin{pmatrix} \psi_{s+1} \\ \psi_s \end{pmatrix} = (-1)^k \mathbf{T}_A^{2p} \begin{pmatrix} \psi_1 \\ \psi_0 \end{pmatrix} \quad (7)$$

which can be easily diagonalised. Choosing  $w = 2|t|\cos\theta$ , for  $\theta/2\pi = p^{-1}$ , with  $p$  an integer, we see that  $\psi_{n \pm p} = \psi_n$  for  $p - A$  sites and hence the amplitude is quasiperiodic in the site index. For other values of  $p$ , the winding number is irrational and  $\psi_{n \pm p} \neq \psi_n$  for any  $p$ . Yet the envelope of the wave function is like an ES. One such wave function for  $E = 0.995|t|$  and  $w = 1.99|t|$  is shown in figure 1. The inset shows  $\psi_n$  up to  $n = 300$  on an enlarged scale. Similar packetted wave functions are obtained in the vicinity of the ES and their 'wave length' keeps on decreasing (Kumar 1990b) as one moves away from  $E_{\text{ex}}$ . The wave function becomes increasingly irregular as the energy is

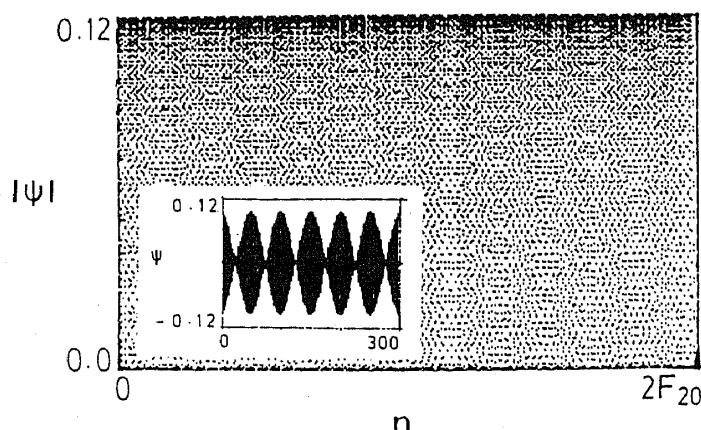


Figure 1. Wave function for  $E = 0.995$  corresponding to 17282th state of a Fibonacci chain of length  $2 \times 10946$ .  $\varepsilon_B = -\varepsilon_A = 0.995$ . Inset shows  $\psi_n$  up to  $n = 300$ .

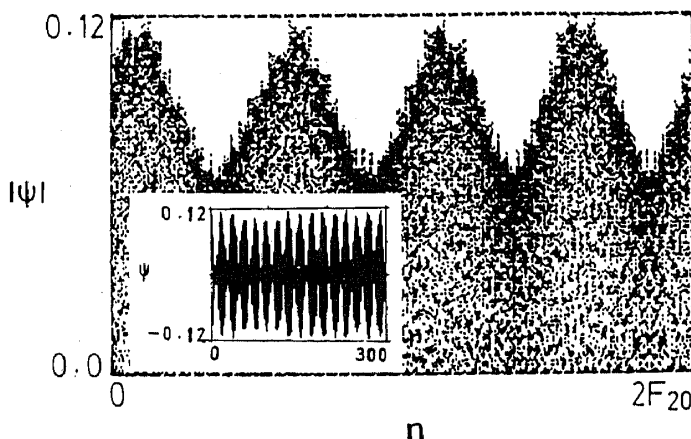


Figure 2. Wave function for  $E = 0.95913049057769$  lying 704 states below the extended state (ES). Inset shows  $\psi_n$  up to  $n = 300$ .

changed. A typical plot of such a wave function for an energy away from  $E_{\text{ex}}$  is shown in figure 2. Although there appears to be some kind of modulation, it is far from regular as can be seen from the inset which shows  $\psi_n$  up to  $n = 300$ . The wave functions at the top edge of the spectrum corresponding to  $N = M = 1$  and  $N = M = 2$ , are shown in figures 3 and 4. Though, the features in both the cases are similar excepting for low lying amplitudes, the scaling properties of the wave functions are different due to this very reason, (see §3C). In the following, we use multifractal method (Halsey *et al* 1986) to characterize the scaling properties of the wave functions.

### 3. Multifractal analysis

#### A. Analytical solution for the extended state

We normalize the wave function over the chain under consideration and choose the probability measure  $P_i = |\psi_i|^2$  with a uniform Lebesgue measure  $\ell = 1/F_r$ . The scaling of the probability measure is taken to be  $P_i \sim \ell^\alpha$ . Then the distribution of the

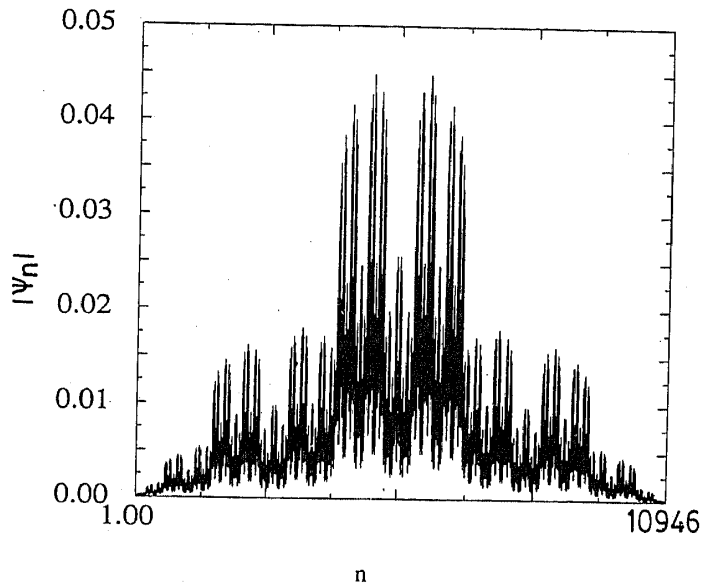


Figure 3. Wave function corresponding to the top edge of a Fibonacci chain of length 10946 with single atom per block

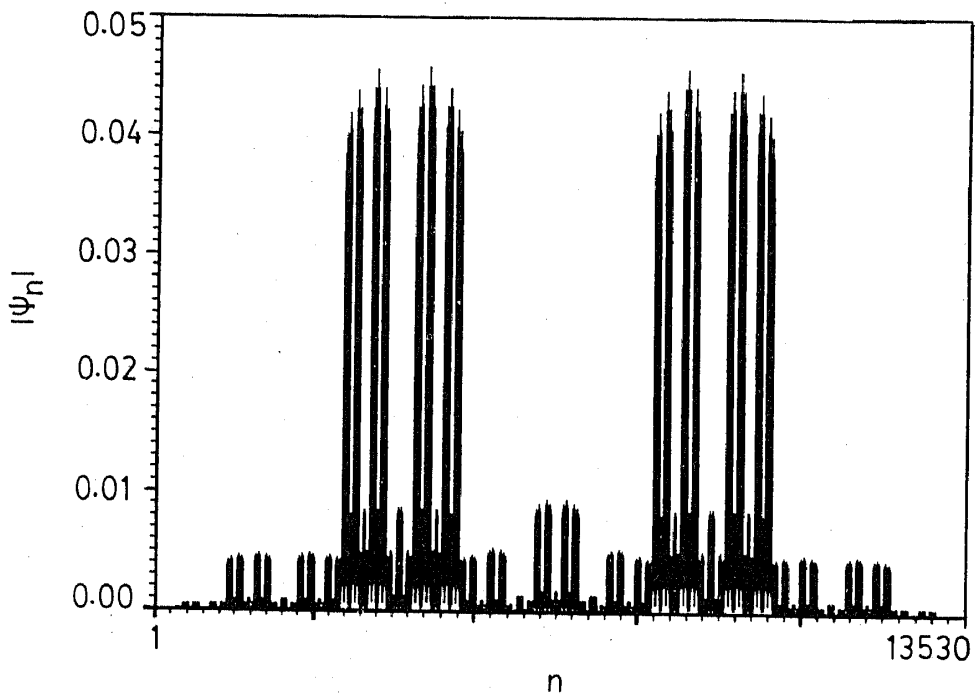


Figure 4. Wave function corresponding to the top edge of a Fibonacci chain of length 6765 with two atoms per block.

singularities  $f(\alpha)$  completely characterizes the wave function. The quantity  $\psi = \sum P_i^q$  scales as  $\ell^\tau(q)$  and is related to  $f(\alpha)$  through

$$\tau(q) = D(q)(q - 1); \quad \frac{d\tau}{dq} = \alpha \quad \text{and} \quad \tau(q) = \alpha q - f(\alpha), \quad (8)$$

where  $D(q)$ 's are the 'generalized dimensions'. For the extended states  $f(\alpha) = \alpha = 1$  and for the localized states  $f(\alpha) = 0$  for  $\alpha = 0$  and  $f(\alpha) = 1$  for  $\alpha \rightarrow \infty$ .

For the wave functions given by (7),  $f(\alpha)$  can be calculated analytically (Ananthkrishna 1989, 1990). Choosing  $\psi_0 = \psi_1 = 1$ , and diagonalizing  $T_A^{2p}$ , we get the unnormalized wave functions at the even and the odd  $A$  sites to be

$$\psi_s(k, p) = -(-1)^k \frac{\sin(4p-1)\theta/2}{\sin\theta/2} \quad (9)$$

and

$$\psi_{s-1}(k, p) = (-1)^k \frac{\sin(4p-3)\theta/2}{\sin\theta/2}. \quad (10)$$

In order to calculate the wave function at  $B$  sites and its normalization constant, we note that the Fibonacci sequence can be represented in terms of three types of sites  $\alpha$ ,  $\beta$  and  $\gamma$  occurring in the sequence  $-\beta\gamma\alpha\beta\gamma\beta\gamma\alpha\beta\gamma\alpha\beta\gamma\dots$  with a frequency of occurrence  $\omega^{-1}:1:1$ , where  $\omega = (1 + \sqrt{5})/2$  is the *golden mean*. This has been studied in the context of diffusion on a Fibonacci chain (Ananthkrishna and Balasubramanian 1988). Both the  $\alpha$  and  $\gamma$  sites host the  $A$  blocks and the  $\beta$  sites host the  $B$  blocks. Further, the  $\beta$  sites always precede the  $\gamma$  sites which implies that the  $\alpha - \gamma$  sub-sequence is adequate for calculating the required sums. Using the above information and appropriate transfer matrices, we get

$$\psi_s = -\psi_{s-1} \quad (11a)$$

and

$$\psi_{s-2}(k, p) = \psi_s(k, p-1) \quad (11b)$$

If we choose  $\mathcal{N} = 2F_{r+1}$ , then using the frequency of occurrence of  $\alpha$ ,  $\beta$  and  $\gamma$  sites, we have

$$\bar{A} \sum_i^{2F_{r+1}} |\psi_i(k, p)|^2 = \bar{A} \left[ \sum_{p, v=1, 2}^{F_{r-1}} |\psi_v(k, p_\gamma)|^2 + \sum_{p, v=1, 2}^{F_{r-2}} |\psi_v(k, p_\alpha)|^2 + \sum_{p, v=1, 2}^{F_{r-1}} |\psi_v(k, p_\gamma)|^2 \right] = 1. \quad (12)$$

These sums can be performed by using the projection technique (Zia and Dallas 1985; Valsakumar and Kumar 1986; Ananthkrishna and Balasubramanian 1988). Consider evaluating the first term in (12). Using (9–11) this can be written (apart from a factor of  $4 \sin^2 \theta/2$ )

$$\sum_{p, (\text{even})}^{F_{r-1}} [2 - \exp\{-i(4p-1)\theta\} - \exp\{i(4p-1)\theta\}]. \quad (13)$$

The projection appropriate to this sequence is shown in figure 5. In the limit of large  $r$ , sums of the form  $\exp(\pm 4ip\theta)$  can be calculated following our earlier work (Ananthkrishna and Balasubramanian 1988)\*. This gives

$$\sum_{p_r}^{F_{r-1}} \exp(\pm 4ip\theta) = \sum_{j, m} \exp(\mp i\phi_{jm}(\sin\phi_{jm})\delta(4\theta \pm K_{jm})/\omega^2\phi_{jm}) \quad (14a)$$

\*Note that  $\gamma$  and  $\beta$  sites are interchanged in the present notation. This amounts to a change in the phase factor.

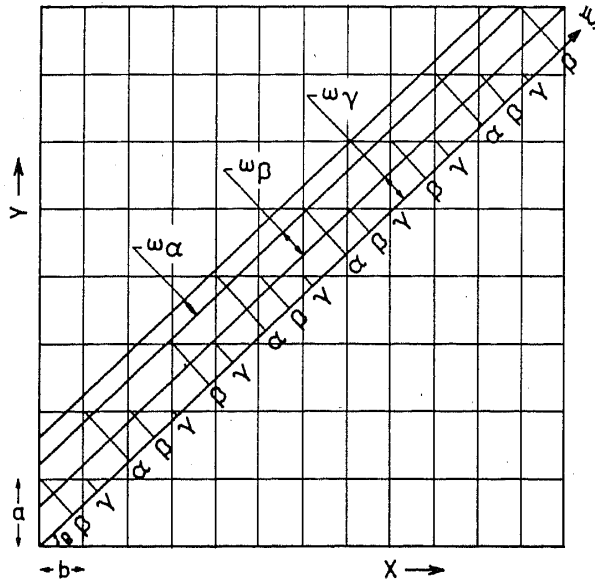


Figure 5. Projection method for obtaining the relevant  $\alpha\beta\gamma$  sequence.  $w_\alpha$ ,  $w_\beta$  and  $w_\gamma$  are the slits widths from which rectangular lattice points are projected on  $\xi$ -axis to obtain the  $\alpha$ ,  $\beta$  and  $\gamma$  sublattices occupied by  $A$ ,  $B$  and  $A$  blocks respectively.

and

$$\sum_{p_z}^{F_{r-2}} \exp(\pm i4p\theta) = \sum_{j,m} \exp\left[\mp i\phi_{jm}\left(\frac{1+4\omega}{\omega}\right)\right] \frac{\sin(\phi_{jm}/\omega)}{\omega^2 \phi_{jm}} \delta(4\theta \pm K_{jm}) \quad (14b)$$

Here  $\phi_{jm} = \pi(m-j)/\omega^2$ , and  $K_{jm} = 2\pi(m+j\omega)/(N\omega + M)$  is the wave vector for the Fibonacci lattice (in our case  $N = M = 2$ ). It is clear that in the large  $r$  limit  $\delta$ -functions do not contribute, since both  $\theta$  and  $K_{jm}$  are in general two different irrational numbers. Thus the first term in (13) gives a dominant contribution equal to  $2F_{r-1}$ . This is same for both the even and the odd terms. An equal contribution arises for the sites. In a similar way, the contribution from the  $\alpha$  sites can be shown to be  $4F_{r-2}$ . Thus,

$$\bar{A} = \sin^2 \theta / 2 \cdot F_{r+1}^{-1}. \quad (15)$$

Therefore, the normalized wave functions, in the limit of large  $r$  are

$$\bar{\psi}_s(k, p) = -(-1)^k \frac{\sin(4p-1)\theta/2}{F_{r+1}^{1/2}}$$

and

$$\bar{\psi}_{s-1}(k, p) = (-1)^k \frac{\sin(4p-3)\theta/2}{F_{r+1}^{1/2}}. \quad (16)$$

With these wave functions one can calculate  $\chi(q) = \sum_i |\bar{\psi}_i(k, p)|^{2q}$ . We can again proceed along similar lines by splitting the sum into three parts as above. It can be shown that for the  $\gamma$  sites the leading contribution is

$$\sum_{p_\gamma}^{F_{r-1}} [2 - \exp[-i(4p_\gamma - 1)\theta] - \exp[\lambda(4p_\gamma - 1)\theta]]^q \sim 2^{q+1} F_{r-1}. \quad (17)$$

An equal contribution comes from the  $\beta$  sites, and a contribution of  $2^{q+1} \cdot F_{r-2}$  arises from the  $\alpha$  sites. (There is an additional contribution arising from equal powers of the exponentials in the binomial expansion. This changes the contribution up to a multiplicative factor which is unimportant). Thus,

$$\chi(q) \sim (2F_{r+1})^{1-q}. \quad (18)$$

Hence, we find

$$\tau(q) \sim q - 1 \quad \text{and} \quad f(\alpha) = \alpha = 1. \quad (19)$$

This is same as expected for a conventional extended wave function. Therefore, the extended type states in quasiperiodic systems have the same generalized dimensions as the Bloch states.

### B. Numerical results and the finite size scaling

*Extended State:* The numerical calculations of  $f(\alpha)$  have been carried out for chains with  $\mathcal{N} = 2F_{r+1}$  sites. Figure 6 shows  $f_r(\alpha)$  for the ES for  $r = 18$  to 23 with  $w = 1.99|t|$  and  $|t| = 1$ . It is clear that even for very large chain lengths  $f_r(\alpha)$  curve is smooth as in the case of a multifractal and far from the anticipated value of  $f(\alpha) = \alpha = 1$ . The convergence is slow but monotonic suggesting the use of finite size scaling. Consider  $\chi_r(q)$  for a chain of length  $F_r$ , then

$$\chi_r(q) \sim \ell^{\tau_r(q)} \sim F_r^{-\tau_r(q)} \sim \omega^{-r\tau_r(q)}. \quad (20)$$

If,  $\tau_r(q) \rightarrow \tau_\infty(q)$ , it is clear that  $\tau_r(q) \sim r^{-1}$ . It may be noted from figure 6 that the sequence of the end points of the curves for  $q > 1$  ( $\alpha < 1$ ) and  $q < 1$  ( $\alpha > 1$ ) having positive and negative slopes, tend to  $f(\alpha) = \alpha = 1$  separately. This should happen for all  $q$ . In contrast, for the self similar states, for each  $q$  there is a limiting value of

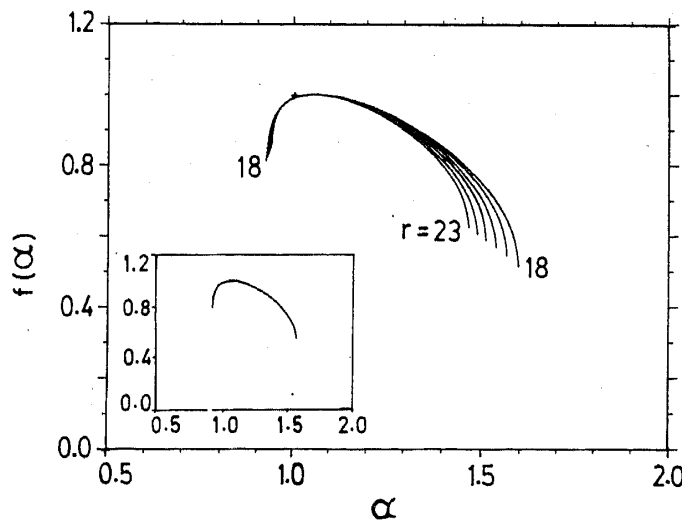


**Figure 6.**  $f_r(\alpha)$  curves for  $r = 16$  to 23 for the ES. + shows the extrapolated value of  $f_\infty(\alpha) = \alpha = 1$ . The inset shows  $f(\alpha)$  behaviour for five successive states (37th to 41st) below the ES.



$f_r(q)$  and  $\alpha_r$ . Due to this, the numerical convergence in the case of extended states is slower than in the case of self-similar states. We have carried out the extrapolation of  $\tau_r(q)$  as a function of  $r^{-1}$  to obtain  $\tau_\infty(q)$  from which we have calculated  $f_\infty(\alpha)$ . This procedure does yield  $f(\alpha) = \alpha = 1$  which is shown as a point in figure 6.

*Cross-over from extended to chaotic states:* When there exist some ES a cross-over behaviour is expected as the other states are critical and generally non-self-similar. To study this cross-over behaviour we have carried out calculations for  $N = M = 2$  for which there are two ES. Since one has to perform the finite size scaling to obtain the multifractal behaviour for an infinite chain, it is important to identify the appropriate states for successive FS. Given a state for the  $r$ th Fibonacci sequence, one convenient way of identifying the corresponding state for successive Fibonacci sequences is by taking the fraction of the states lying between that state and the ES. This is suggested by the observation that the ES itself lies at a specific percentage of states from the upper most state. This establishes a correspondence between a state with a specific energy and the fraction of states below the ES. Using this identification, we have studied the  $f(\alpha)$  spectrum for several consecutive states in the neighbourhood of the ES. We find that for several successive states the  $f(\alpha)$  curves are indistinguishable as can be seen from the inset of figure (6). This implies that  $f_r(\alpha)$  is a smooth function of the state number in the vicinity of the ES.  $\tau_r(q)$  can be extrapolated for such and we find that the  $f(\alpha)$  behaviour is nearly the same as for the ES. Away from the ES the  $f(\alpha)$  spectrum for successive states is different. In such cases keeping the same fraction of states for successive FS, the extrapolated  $\tau(q)$  led to violation of the convexity property of  $f(\alpha)$  over a range of  $q$ . This range of  $q$  increases as we go further away from the ES and behaviour of  $f_r(\alpha)$  for various  $r$  is no longer monotonic. A typical such plot is shown in figure (7) for a state  $\sim 4.64\%$  below the ES. The above behaviour of  $f(\alpha)$  for states in the neighbourhood of the ES as against the states which are far away is due to the fact that in the neighbourhood of the ES, gaps are small and the nature of wave function changes smoothly, whereas the magnitude of the gaps increases as we go away from the ES and the nature of the wave functions changes abruptly across the gap. We consider the breakdown of the extrapolation of

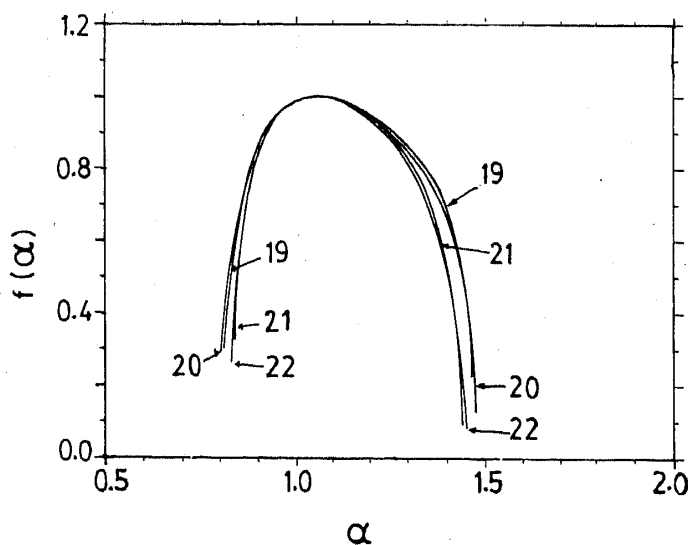


Figure 7. The  $f_r(\alpha)$  curves for  $r = 19$  to 22 for a state which is  $\sim 4.64\%$  states below the ES.

$f(\alpha)$  as the signature of a chaotic state. Fujiwara *et al* (1989) have arrived at a similar conclusion for a FS with one atom per cell. The cross-over is gradual in the sense that the region of  $q$  where the convexity property of  $f(\alpha)$  is violated increase gradually.

### C. Wave functions at band edges

Fujiwara *et al* (1989) have studied the wave functions at the band edge in the case of the off-diagonal model with a single atom per site. Kohmoto *et al* (1987) have shown that wave functions at the band edges correspond to a two cycle of the trace map with  $x(y) = \pm J \pm (J^2 + J)^{1/2}$ , with  $J = \{+3 + (25 + 16I)^{1/2}\}/8$ . For single atom per block, though for a given  $r$ , the multifractal behaviour of the wave functions are different for different edges, the finite size scaling leads to the same multifractal spectrum as shown in the inset of figure (8). In the case of more than one atom per cell, the invariant  $I$  is energy dependent (eq. (5)) and therefore the wave functions corresponding to different edges have different multifractal spectrum. This is shown in figure (8) for wave functions corresponding to the lowest ( $L$ ) and the highest ( $H$ ) energy of the spectrum. For both these states, the wave functions exhibit self-similarity and correspond to a two cycle of the trace map  $x \rightarrow y \rightarrow x$ . The extent of  $\alpha$  in this case is quite different as compared to the case of  $N = M = 1$ . The maximum value of  $\alpha$  is controlled by the smallest amplitude of the wave function. Since this is smaller for the case of the wave function corresponding to two atom per block than one atom per block (see figures 3 and 4), the maximum value of  $\alpha$  is larger than in the case of one atom per block.

### D. The Poincare map

A study of the Poincare maps of the wave functions provides another way of visualizing the change in the nature of the wave functions. Given a time series  $x(t)$  one simple

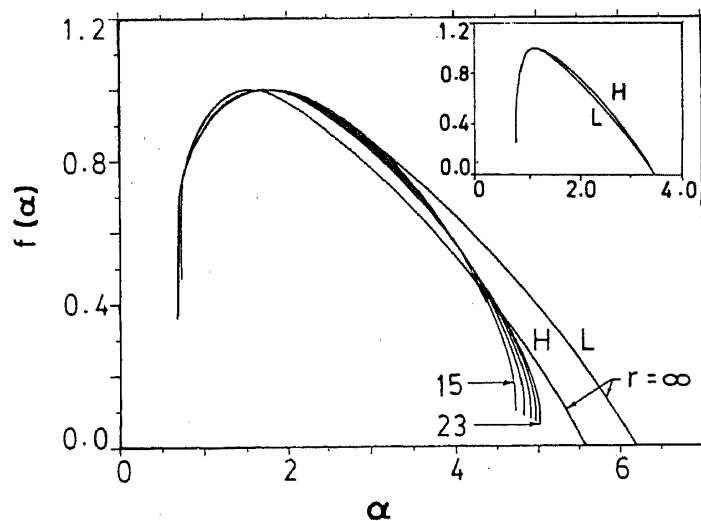


**Figure 8.**  $f_r(\alpha)$  for  $r = 2x + 1$ ,  $x = 7$  to  $11$  and  $f_\infty(\alpha)$  for the wave function at the upper edge ( $H$ ) with  $E = 2.37744477546\dots$   $f_\infty(\alpha)$  for the lower edge ( $L$ ) with  $E = -2.5404156553\dots$  is also shown.  $f_\infty(\alpha)$  for both the upper ( $H$ ) and the lower ( $L$ ) edges for  $N = M = 1$  are shown in the inset.

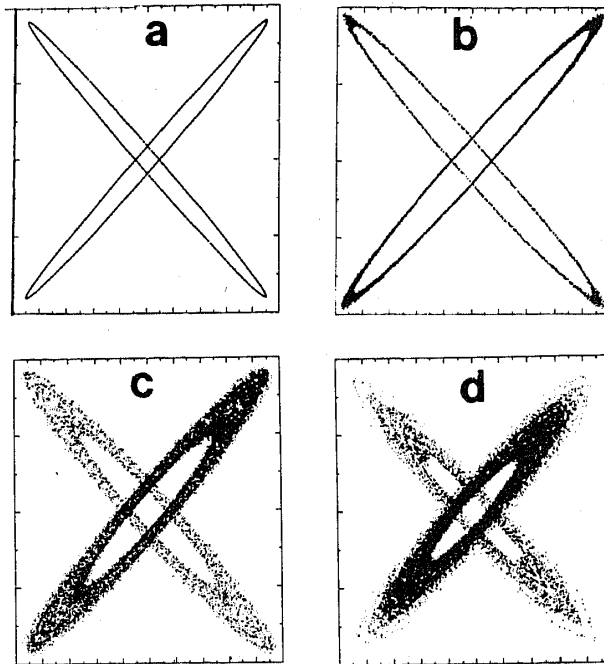


Figure 9. The Poincaré map of  $\psi_{n+1}$  vs  $\psi_n$  for  $r = 20$  corresponding to (a) the extended state, (b) 287, (c) 704 and (d) 1017 states below the ES respectively.

way to obtain the Poincaré map is to plot  $x(t)$  at time  $t = t_n$  vs  $x(t)$  at  $t = t_{n+1}$ . In the present case the site index  $n$  takes the role of  $t_n$  and  $\psi_n$  vs  $\psi_{n+1}$  is plotted. Figures (9a–d) show the Poincaré maps of the wave functions for the extended states and three states in the vicinity of the ES for  $r = 20$ . The closed curve in figure (9a) is due to the quasiperiodic nature of the ES. The two branches have density of points in the ratio of  $\omega:1$  corresponding to the fraction of the  $A$  to the  $B$  sites. As we go away from the ES the trajectories increasingly spread out into the  $X - Y$  plane suggesting an increasing degree of randomness of the wave functions. The  $f(\alpha)$  curve of figure (9b) shown in the inset of figure (6) is nearly the same as for the ES. Figure (9c,d) are already in the chaotic regime in the sense that it is not possible to extrapolate  $f_r(\alpha)$  to obtain  $f(\alpha)$ . The  $f_r(\alpha)$  curve corresponding to figure (9d) is shown in figure (7) which shows no monotonicity. This corroborates the results obtained from the multifractal analysis.

#### 4. Summary

We have carried out a multifractal analysis of the wave functions for the Fibonacci sequence with one or two atoms per cell. In the case of two atoms per cell, the extended type states have been shown to have the same signature as Bloch states with  $f(\alpha) = \alpha = 1$ . Also several states in the vicinity of the extended state have similar behaviour. This suggests that the frequency dependent conductivity for these energies may be close to that for the periodic systems. The other states show two types of behaviours (1) the self-similar states at the band edges for which  $f(\alpha)$  has a monotonic dependence on the system size and (2) chaotic states which do not exhibit such a monotonicity.

A similar analysis (Thakur *et al* 1989) has been extended to the study of the mobility edge arising in the generalized Harpers model with  $V(n) = \lambda \cos(2\pi\omega n^\nu)$ ,  $0 < \nu < 2$ .

### Acknowledgements

We are thankful to the referee for bringing to our attention the work of Hiramoto and Kohmoto. Part of the work was performed at ICTP, Trieste and we are thankful to Prof. Abdus Salam, the IAEA and UNESCO for their hospitality.

### References

- Ananthkrishna G and Kumar V 1988 *Phys. Rev. Lett.* **60** 1586  
 Ananthkrishna G and Balasubramanian T 1988 *Bull. Mater. Sci.* **10** 77  
 Ananthkrishna G 1990 *J. Phys. Condens. Matter* **2** 1343 (see also Ananthkrishna G 1989 *Phase transitions* Vol. 16/17 589)  
 Delyon K and Petritis D 1986 *Commun. Math. Phys.* **103** 441  
 Evangelu S N 1987 *J. Phys.* **C20** L295  
 Fujiwara T, Kohmoto M and Tokihiro T 1989 *Phys. Rev.* **B40** 7413  
 Halsey T C, Jensen M H, Kadanoff L P, Procaccia I and Shraiman B I 1986 *Phys. Rev.* **A33** 1141  
 Hentschel H G E and Procaccia I 1983 *Physica* **D8** 835  
 Hiramoto H and Kohmoto M 1989 *Phys. Rev.* **B40** 8225  
 Kohmoto M, Kadanoff L P and Tang C 1983 *Phys. Rev. Lett.* **50** 1870  
 Kohmoto M, Sutherland B and Tang C 1987 *Phys. Rev.* **B35** 1024  
 Kumar V and Ananthkrishna G 1987 *Phys. Rev. Lett.* **59** 1476  
 Kumar V 1990a *J. Phys. Condens. Matter* **2** 1349  
 Kumar V 1990 in *Quasicrystals* (eds) M V Jaric and S Lundquist (Singapore: World Scientific)  
 Mato G and Caro A 1987 *J. Phys.* **C20** L717  
 Nori F and Rodriguez P 1986 *Phys. Rev.* **B34** 207  
 Ostlund S, Pandit R, Rand D, Schellnhuber H J and Siggia E D 1983 *Phys. Rev. Lett.* **50** 1873  
 Pietronero L, Siebesma A P, Tosatti E and Zennetti M 1987 *Phys. Rev.* **B36** 5635  
 Siebesma A P and Pietronero L 1987 *Europhys. Lett.* **4** 597  
 Suto A 1989 *J. Stat. Phys.* **56** 525  
 Thakur P K, Brouers F and Ananthkrishna G 1989 ICTP Preprint IC/89/350  
 Valsakumar M C and Ananthkrishna G 1987 *J. Phys.* **C20** 9  
 Valsakumar M C and Kumar V 1986 *Pramana - J. Phys.* **26** 215  
 Zia R K P and Dallas W 1985 *J. Phys.* **A18** L341